Published in final edited form as:
Prostate. 2014 November ; 74(15): 1506–1520. doi:10.1002/pros.22868.

Activation of Wnt/β-catenin signaling in a subpopulation of murine prostate luminal epithelial cells induces high grade prostate intraepithelial neoplasia

Kenneth C. Valkenburg[1], **Xiuping Yu**[2], **Angelo M. De Marzo**[3], **Tyler Spiering**[1,4], **Robert J. Matusik**[2], and **Bart O. Williams**[1]

[1]Center for Skeletal Disease & Tumor Metastasis, Van Andel Research Institute, 333 Bostwick Ave. NE, Grand Rapids, MI 49503

[2]Department of Urological Surgery, Vanderbilt University Medical Center, Nashville, TN 37232-2765

[3]Department of Pathology, Johns Hopkins University School of Medicine, 600 N. Wolfe St., Baltimore, MD 21287

[4]Wayne State University School of Medicine, 540 East Canfield, Detroit, MI 48201

Abstract

Background—Wnt/β-catenin signaling is important for prostate development and cancer in humans. Activation of this pathway in differentiated luminal cells of mice induces high-grade prostate intraepithelial neoplasia (HGPIN). Though the cell of origin of prostate cancer has yet to be conclusively identified, a castration-resistant Nkx3.1-expressing cell (CARN) may act as a cell of origin for prostate cancer.

Methods—To activate Wnt/β-catenin signaling in CARNs, we crossed mice carrying tamoxifen-inducible Nkx3.1-driven Cre to mice containing loxP sites in order to either conditionally knock out adenomatous polyposis coli (Apc) or constitutively activate β-catenin directly. We then castrated and hormonally regenerated these mice to target the CARN population.

Results—Loss of Apc in hormonally normal mice induced HGPIN; however, after one or more rounds of castration and hormonal regeneration, Apc-null CARNs disappeared. Alternatively, when β-catenin was constitutively activated under the same conditions, HGPIN was apparent.

Conclusion—Activation of Wnt/β-catenin signaling via Apc deletion is sufficient to produce HGPIN in hormonally normal mice. Loss of Apc may destabilize the CARN population under regeneration conditions. When β-catenin is constitutively activated, HGPIN occurs in hormonally regenerated mice. A second genetic hit is likely required to cause progression to carcinoma and metastasis.

Correspondence: Kenneth C. Valkenburg, ken.valkenburg@vai.org, t: 616-234-5568, f: 616-234-5309; Xiuping Yu, Xiuping.yu@vanderbilt.edu, t: 615-343-1902; Angelo De Marzo, ademarz@jhmi.edu, t: 410-614-5686; Tyler Spiering, tspierin@med.wayne.edu, t: 616-540-2029; Robert J. Matusik, Robert.matusik@vanderbilt.edu, t: 615-343-1902, f: 615-322-8990, Bart O. Williams, bart.williams@vai.org, t: 616-234-5308, f: 616-234-5309.

Disclosure Statement
The authors have no financial conflicts of interest to disclose.

Keywords

Apc; Beta-catenin; Wnt; Nkx3.1; CARNs; mouse model

Introduction

Prostate cancer is the most diagnosed non-skin cancer and is responsible for the second-most cancer-related deaths in U.S. men [1]. Many prostate cancer cases are relatively indolent, resulting in a 5-year survival rate approaching 100% [1]. However, once prostate cancer becomes metastatic, 5-year survival rates are an abysmal 30% [1]. There is no cure for metastatic prostate cancer, and few experimental models accurately recapitulate the tumorigenic progression and the metastatic cascade that is seen in human patients. While the number of genetically engineered mouse models is growing [2, 3], better experimental prostate cancer models are needed to represent both indolent and aggressive prostate cancer.

Prostate cancer is a genetically and etiologically heterogeneous disease [4, 5]. Wnt/β-catenin signaling is crucial for regulating prostate development and is generally inactive in normal differentiated prostate cells [6-9]. Active Wnt/β-catenin signaling is associated with human prostate cancer, and correlates with prostate cancer progression [10, 11]. Elevated nuclear β-catenin expression is found in approximately 20% of advanced prostate tumors and 85% of skeletal bone metastases [12]. We have previously shown that prostate-specific activation of β-catenin in mouse models causes high grade prostate intraepithelial neoplasia (HGPIN), the precursor to prostate cancer [13], and the activation of both SV40 large T-antigen and Wnt signaling induces carcinoma [14]. In addition, while it is well known that inactivation of APC causes intestinal tumors [15], it is also associated with prostate cancer [16-19]. Most of the evidence linking APC to human prostate cancer is that of promoter hypermethylation and subsequent reduced expression [19, 20]. We have previously shown that deleting Apc in murine prostate epithelial cells induces β-catenin signaling, leading to high-grade intraepithelial neoplasia (HGPIN) with infrequent micro-invasive characteristics and castration resistance [21].

The prostate comprises three main epithelial cell types: basal, luminal, and neuroendocrine. The development and growth of the prostate gland is regulated by androgen signaling, primarily through the androgen receptor (AR). Prostate cancer generally depends on androgen signaling as well, hence the use of androgen deprivation therapy (ADT) as a treatment for advanced prostate cancer. Prostate cancer can become resistant to ADT (castration resistance). A definitive cell of origin for human prostate cancer has not been identified. In mice, models exist that suggest that prostate cancer can arise from either basal or luminal cells [22-25]. A population of luminal epithelial cells has been identified in the mouse that is castration resistant and is able to differentiate into both luminal and basal cells [23]. These cells express the homeobox gene, *Nkx3.1*, and are referred to as castration resistant Nkx3.1-expressing cells (CARNs) [23]. The *Nkx3.1* gene promoter was used to drive Cre recombinase expression and conditionally delete phosphatase and tensin homolog (Pten) in the CARN population, which resulted in HGPIN and carcinoma, suggesting that the CARN population is a cell of origin for prostate cancer [23].

We utilized either floxed Apc mice [21] or mice carrying an allele of the β-catenin gene (*Ctnnb1*) in which the third exon was flanked by loxP sites (floxed) [26]. After exposure to Cre recombinase, this latter allele expressed a non-degradable version of the β-catenin protein. These alleles were individually crossed to Nkx3.1-driven Cre transgenic mice [23] to activate β-catenin in the luminal population, and then specifically in the CARN population through castration and hormonal regeneration. We show that this resulted in accumulation of β-catenin, hyperplasia, and regions of carcinoma that are castration resistant. Interestingly, we also show that one or more rounds of castration and hormonal regeneration in the Apc conditional knockout resulted in loss of this phenotype.

Materials and methods

Generation of mice

Apc^{flox} [21], $Ctnnb1^{lox(ex3)}$ [26], $Nkx3.1^{CreERT}$ [23], *mT/mG* [27], and PB^{Cre4} mice [28] have all been previously described. All animals were used in protocols that were reviewed and approved by Institutional Animal Care and Use Committees of the Van Andel Research Institute and Vanderbilt University. To generate Apc^{cKO} mice, we crossed $Nkx3.1^{CreERT}$ heterozygous mice (transgenic allele plus wild-type allele, or tg/+) with mice homozygous for a floxed allele of *Apc* (flox/flox) to generate $Nkx3.1^{CreERTtg/+};Apc^{flox/+}$ mice. We then crossed these mice together to generate homozygous mutant $Nkx3.1^{CreERTtg/+};Apc^{flox/flox}$ mice. Mice wild-type for Cre ($Nkx3.1^{CreERT+/+};Apc^{flox/flox}$) were subjected to the same experimental conditions as the mutant mice and were used as controls. To generate $Bcat^{cAct}$ mice, we crossed $Nkx3.1^{CreERTtg/+}$ with mice homozygous for a floxed allele of *Ctnnb1* (exon 3 flox/flox) to generate $Nkx3.1^{CreERTtg/+};Ctnnb1^{lox(ex3)}$ mice. To generate $Nkx3.1^{CreERT}mT/mG$ mice, we crossed $Nkx3.1^{CreERTtg/+}$ mice with *mT/mG* mice homozygous for the knock-in *mT/mG* allele (ki/ki) to generate mice heterozygous for both Cre and mT/mG ($Nkx3.1^{CreERTtg/+};mT/mG^{ki/+}$). The same strategy was used to generate $PB^{Cre4}mT/mG$ mice. For genotyping of all mice, DNA was prepared from tail biopsies using sodium hydroxide extraction [29]. PCR-based strategies were then used to genotype these mice [28, 30].

Tamoxifen administration

Tamoxifen (Sigma T5648) was dissolved at 20 mg/mL in a 9:1 mixture of corn oil and ethanol the same day of administration to mice. This tamoxifen mixture (500 μL) was administered to mice via oral gavage once per day for 2 consecutive days.

Allele-specific and quantitative reverse transcriptase PCR

To confirm that exon 14 of *Apc* had been deleted in the prostate of mutant NKAP mice, DNA was isolated from whole prostate lobes using the Qiagen DNeasy kit (69504), and PCR amplification was done to amplify wild-type, floxed, or deleted alleles using previously described primers [30]. For qualitative or quantitative RT-PCR, RNA was removed from mouse prostate using Trizol, centrifuged with chloroform to separate out the aqueous RNA phase, and then RNA was ethanol precipitated and purified using the Qiagen RNeasy kit (74034).

Histology and immunohistochemistry

For hematoxylin (Sigma MHS16) and eosin (Sigma HT110216) staining and immunohistochemistry, tissues were fixed in 10% neutral buffered formalin (NBF) for 24-48 hours, embedded in paraffin, and sectioned at 5 μm thickness. Immunohistochemical staining was optimized using the Discovery XT System (Ventana, Tuscon, AZ). The following antibodies were used for immunohistochemistry: β-catenin (Cell Signaling Technology 9562), activated β-catenin (Cell Signaling 8814), Ki67 (Spring Biosciences M306), Apc (Santa Cruz sc-896 C-20), cyclin D1 (Thermo Scientific RM-9104-R7), Foxa2 (HNF-3β, Santa Cruz sc-9187), p63 (Santa Cruz sc-8343), cleaved caspase 3 (Cell Signaling 9664), AR (Abcam ab133273), cytokeratin 14 (Covance PRB-155P), cytokeratin 8 (Spring Biosciences E18400 for IHC or Developmental Studies Hybridoma Bank for IF), c-myc (Epitomics 1472-1), and Taz (Abcam ab110239).

Hormone ELISA

Upon dissection of mice, approximately 500 μL of blood was removed via intracardiac puncture, mixed with 5 μL of 0.5 M EDTA, pH 8.0, and then centrifuged at 6,000×g for 6 minutes. Approximately 200 μL of serum was removed from the top layer and stored at −80°C. This serum was used in the Cayman Chemical testosterone EIA kit or estradiol EIA kit to determine hormone levels. The student's T-test was used to assess potential statistical differences between groups.

Castration and testosterone re-administration

For surgical castration, a single 1 cm longitudinal incision was made in the skin and peritoneum anterior to the preputial gland. The epididymal fat pad, vas deferens, and both testes were removed via cauterization. The peritoneal incision was sutured shut, and the skin was closed with wound clips. Wound clips were removed 14 days post-surgery. Post-castration mice showed no signs of infection. Testosterone (Sigma T1500) was administered to mice via semipermeable silastic tubes subcutaneously inserted into the dorsal mid-trunk region of the mice. This method has been previously described [31]. These tubes were removed when required for testosterone removal.

Imaging and counting of GFP-positive cells in mT/mG mice

Tissues were removed from *mT/mG* mice, fixed in 10% NBF overnight, and then placed in 30% sucrose at 4 °C overnight to extract any remaining water. Tissues were then cryo-embedded in OCT medium, frozen at −80 °C, and subsequently cryo-sectioned at 5 to 10 μm thickness. Tissues were stained with DAPI for 10 minutes at room temperature prior to cover-slipping and imaging on a Zeiss 410 or Nikon A1 confocal microscope. GFP-positive cells in the confocal images were counted using FIJI software. The student's T-test was used to assess potential statistical differences between groups.

Nuance microscopy quantification

Images were taken on a Nuance microscope, and were un-mixed for brown stain and blue (hematoxylin) stain. Identical thresholds were used to quantify the number of positively stained pixels for either the IHC stain (e.g. Ki67) or hematoxylin. Hematoxylin-positive

nuclei represented the denominator, and IHC-stained nuclei represented the numerator. The student's T-test was used to assess potential statistical differences between groups.

Results

HGPIN in the Apc^{cKO} model

In our previous study, we conditionally deleted Apc in luminal cells of the murine prostate using the *Probasin*^{Cre4} transgene (*PB*^{Cre4}) [21, 28]. The *Apc*^{flox} mouse has been described previously (Supplemental Figure 1a) [21]. When exon 14 of the *Apc* gene, which is flanked by loxP sites ("floxed") is deleted, Apc is rendered inactive. In the present study, we induced recombination of *Apc* with *Nkx3.1*^{CreERT} [23]. In this model, the Cre recombinase gene is fused to a mutated version of the estrogen receptor (ER) ligand-binding domain that encodes a protein that no longer responds to endogenous estradiol and is only activated by tamoxifen (Supplemental Figure 1b). We crossed *Nkx3.1*^{CreERT} mice with *Apc*^{flox} mice to generate *Nkx3.1*^{CreERT}*Apc*^{flox} mice, which we will refer to as either Apc^{flox} (*Nkx3.1*^{CreERTwt}*Apc*$^{flox/flox}$) or Apc^{cKO} (*Nkx3.1*$^{CreERTtg/+}$*Apc*$^{flox/flox}$) throughout the remainder of this paper. We treated these mice with tamoxifen via oral gavage at 12 weeks of age (Figure 1a) and showed via allele-specific PCR that the Apc gene was indeed deleted in the prostate, but not in any of the non-prostatic tissues we tested (Figure 1b). We showed via immunohistochemistry (IHC) and real-time PCR (RT-PCR) that Apc is lost at the protein and RNA level in Apc^{cKO} mice and that β-catenin protein levels increase in response to Apc deletion (Figures 1c-d). In the same samples, we performed quantitative RT-PCR (qRT-PCR) and found that the gene encoding β-catenin (*Ctnnb1*) and the Wnt target genes *Axin2*, and *c-Myc* were all significantly up-regulated upon Apc loss (Figure 1e). Surprisingly, the gene encoding Cyclin D1 (*Ccnd1*) was down-regulated in the Apc^{cKO} prostate cells relative to Apc^{flox} cells (Figure 1e). To determine the specificity of *Nkx3.1*^{CreERT} recombinase activity, we crossed *Nkx3.1*^{CreERT} mice to double fluorescent reporter *mT/mG* mice [27]. This mouse ubiquitously expresses the red fluorescent protein Tomato in the membrane of cells. Upon Cre activation, Tomato is excised and green fluorescent protein (GFP) expression is induced via the excision of a lox-stop-lox site upstream of GFP (Supplemental Figure 1c). We saw GFP expression in whole prostates from *Nkx3.1*$^{CreERTtg/+}$*mT/mG*$^{ki/ki}$ mice (Supplemental Figure 1d) and following cryo-section (Figure 1f). To determine whether *Nkx3.1*^{CreERT} recombinase was active in any other tissues after tamoxifen treatment, we cryosectioned tissues from throughout the body and found GFP expression only in the bulbourethral gland (Supplemental Figures 1e-f); Nkx3.1 expression in this gland had been reported previously [32]. We did not, however, find a phenotype in these glands (data not shown). We quantified the percentage of GFP-positive cells in a representative portion of prostate tissue and found that *Nkx3.1*^{CreERT} was active one day after tamoxifen treatment in an average of 22% of luminal cells in the anterior prostate of tamoxifen-treated mice, versus an average of 59% in *PB*^{cre4}*mT/mG* anterior lobes by 4 weeks of age (Figure 1g, Supplemental Figures 1g-h). We found GFP expression in the oldest mice we assessed, 7 months after tamoxifen treatment (data not shown), indicating that once recombination occurs in a cell, as expected, its progeny retain the recombined portion.

HGPIN in tamoxifen-treated, hormonally normal Apc^{cKO} mice

We treated mice with tamoxifen at 3 months of age, and we monitored them to 4 months, 7 months, 10 months, or 13 months of age. In these hormonally normal mice, we assumed that CARNs were present within the luminal population, but that these would not be the only cells in which *Apc* was deleted (as *Nkx3.1* is expressed in both CARN and non-CARN luminal cells under hormonally normal conditions). At 4 months of age, Apc^{cKO} mice displayed regional hyperplasia, increased β-catenin expression, and an increase in Ki67 staining (data not shown). We did more analysis at 7 months of age, to compare them to the *PB^{Cre4}Apc^{flox}* model that we had previously published [21]. At this and other time points, the most severe phenotype was restricted to the anterior lobe of the prostate; the ventral and dorsolateral lobes showed little evidence of hyperplasia or any aspects of PIN (Supplemental Figure 2a). Because the *Nkx3.1^{CreERT}* construct is a knock-in that creates one null *Nkx3.1* allele, we checked *Nkx3.1$^{CreERTtg/+}$Apc^{wt}* prostate tissue and found no evidence of hyperplasia or PIN (Supplemental Figure 2b). However, it is possible that the combination of loss of one *Nkx3.1* allele along with homozygous deletion of *Apc* contributes to the phenotype [33]. Apc^{cKO} mice at 7 months of age displayed glandular hypercellularity in which gland lumens were often completely filled with cells with mild nuclear enlargement and occasional mild nucleolar enlargement, but no areas of invasion or metastasis, consistent with a diagnosis of HGPIN (Figure 2) [34]. These mice also showed increased cytoplasmic and nuclear β-catenin staining, as well as increased nuclear activated β-catenin (non-phosphorylated Ser33/37/Thr41 residues) with a correlative increase in the proliferation marker Ki67 and cell cycle marker cyclin D1 (Figure 2). Unexpectedly, cyclin D1 RNA levels decrease while protein levels increase (see Figure 1e and Figure 2). Apc^{cKO} mice also expressed more nuclear and cytoplasmic c-myc relative to Apc^{flox} mice (Figure 2). In control mice, β-catenin was only detected in the cellular membrane, and very few cells were positive for Ki67, cyclin D1 or c-myc. The increase in Ki67 was quantified and found to be statistically significantly higher in Apc^{cKO} mice (Supplemental Figure 3a).

There was a modest increase in cleaved caspase 3 expression, indicative of a higher rate of apoptosis in regions of Apc^{cKO} mice (Figure 3). To determine the epithelial nature of the affected cells in Apc^{cKO} mice, we stained for luminal marker cytokeratin 8 (CK8), which was confined to the luminal compartment in both Apc^{flox} and Apc^{cKO} (Figure 3). We also stained for androgen receptor (AR) and found it to be expressed primarily in the luminal compartment of both Apc^{flox} and Apc^{cKO} mice and in a small percentage of basal cells (Figure 3). Surprisingly, AR expression was present in a higher percentage of nuclei from Apc^{cKO} mice relative to Apc^{flox}, although the amount of AR protein decreased over time (Supplemental figure 3b). We also stained for the basal cell markers cytokeratin 14 (CK14) and p63, which were localized nearly exclusively (CK14) and exclusively (p63) to basal cells as expected. The vast majority of the atypical β-catenin nuclear positive PIN lesional cells were luminal in location and stained positively for CK8 and negatively for CK14. However, a small percentage (~4%) of presumed lesional cells co-expressed CK8 and CK14 in small clusters (Figure 3 and Supplemental figure 3c), similar to what was found in the *PB^{Cre}Apc^{flox}* mice [21]. We also found that Apc^{cKO} cells had increased Foxa2 expression, which is up-regulated by β-catenin [14, 35] (Figure 3). Foxa2 and Wnt/β-catenin signaling are active in early embryonic buds of the prostate [8, 36], and Foxa2 is also active in

prostatic neuroendocrine cells. Finally, we found that Apc^{cKO} cells had increased Taz expression (Figure 3), which could indicate a reduction of Hippo signaling and concurrent tissue growth [37], or could simply be a marker of increased β-catenin expression [38]. Either way, Taz activity is an indicator of increased cellular proliferation and growth [39]. To assure that estrogen levels were not being affected by addition of tamoxifen, we performed an estradiol ELISA and found no significant change (Supplemental Figure 3d). We also performed a testosterone ELISA and found no significant change between tamoxifen-treated mice relative to control mice (Supplemental Figure 3e).

In Apc^{cKO} mice at 10 and 13 months, HGPIN was apparent but did not seem to progress to invasive disease (data not shown). However, Apc^{cKO} mice developed large liver tumors at 10 months of age with 100% penetrance (Supplemental Figure 4a). We conducted allele-specific PCR on liver tumor tissue and found no evidence of *Apc* deletion; the same assay was performed on lung, lymph node, and bone marrow tissue found no evidence of deletion (Supplemental Figure 4b). AR IHC on these tissues showed no evidence of AR expression anywhere but the prostate (Supplemental Figure 4c). These observations are cinsistent with previous observations in our $PB^{Cre}Apc^{flox}$ model [21]. These data indicate that no secondary tumor sites were present in Apc^{cKO} mice.

A small population of Apc^{cKO} cells survived castration but did not proliferate

We castrated mice at 2 months of age and then treated them with tamoxifen at 3 months to determine whether tumorigenesis could occur from the CARN population without hormonal regeneration (Figure 4a). Prostates in castrated mice shrunk to approximately $1/10^{th}$ the size of a normal prostate (Figure 4b), and testosterone in the sera of castrated mice was negligible (Supplemental figure 3e). PCR for Apc showed deletion did indeed occur in castrated and tamoxifen-treated mice, though at a lesser level than in tamoxifen-only mice (data not shown). Upon mT/mG analysis, recombination still took place in approximately 12% of luminal cells (Figures 4c and 1g). There was no discernible difference in AR staining, and no detectable phenotype by histological analysis of tissues from the mutant mice (Figures 4c-d). There were few cells that showed cytoplasmic β-catenin staining in the mutants (we concluded that these cells were CARNs), but no difference was seen in Ki67 or AR staining (Figures 4d). These data indicate that while Apc is being deleted in a small population of luminal cells of castrated mice (likely CARNs), the loss of Apc is insufficient to drive tumorigenesis in these cells.

Cells in Apc^{cKO} mice continue to proliferate upon castration after tamoxifen treatment

To determine whether the HGPIN phenotype seen in Apc^{cKO} mice would persist following castration, we treated mice at 3 months of age with tamoxifen, and then castrated them three months later (Figure 5a). mT/mG analysis showed that recombination took place in approximately 7% of luminal cells following castration (Figures 5b and 1g). Apc^{cKO} prostates appeared larger upon dissection than their Apc^{flox} counterparts (data not shown). A small population of cells retained β-catenin cytoplasmic staining, and there was significantly more Ki67 staining in the Apc^{cKO} mice relative to Apc^{flox} controls (Figures 5b-c). These data suggest that tamoxifen treatment causes *Apc* deletion associated with β-catenin accumulation and nuclear localization (as seen in hormonally normal tamoxifen-only mice),

and that castration causes these phenotypes to deteriorate. This process takes time, as evidenced by higher proliferative rate of cells in Apc^{cKO} mice, indicating slight castration resistance.

HGPIN phenotype disappears after one or more cycles of hormonal regeneration in Apc^{cKO} mice

In the Wang *et al.* paper that first reported the use of *Nkx3.1*^{CreERT} mice, they selected for a CARN-rich population by castrating mice, treating with tamoxifen, and then readministering testosterone to expand a CARN population that had the tumor suppressor phosphatase and tensin homolog (Pten) deleted [23]. We followed a similar strategy with our model (Figure 6a). Following hormonal regeneration, prostates were the same size as a tamoxifen-only, hormonally normal prostate (Figure 6b). Testosterone levels in regenerated mice increased approximately 20-fold over hormonally normal mice (Supplemental Figure 3e). Upon mT/mG analysis, there were significantly more GFP-positive luminal cells in the regenerated mice relative to the tamoxifen-only group (Figures 6c and 1g). However, this expansion of the CARN population did not translate to the Apc^{cKO} mice. After one round of castration and regeneration, there was no evidence of hyperplasia or HGPIN, cytoplasmic or nuclear β-catenin expression, or differential Ki67 expression (Figure 6c). The prostates from these Apc^{cKO} mice appeared normal. To determine whether multiple rounds of castration and regeneration expand the Apc^{cKO} CARN population, we castrated, regenerated, removed testosterone, and then regenerated again in a cyclic fashion (Figure 6d). In the mT/mG mice, GFP-positive cells decreased (Figures 6e and 1g) and the prostate once again appeared normal, similar to the mice that had undergone one cycle of regeneration (Figure 6e). The Apc^{cKO} cell population appeared to disappear after one or more cycles of castration and hormonal regeneration. These data suggest that although the Apc^{cKO} CARN population is indeed resistant to apoptosis under castration conditions, increased proliferation is not associated with androgen-mediated regeneration.

HGPIN in tamoxifen-treated, hormonally regenerated $Bcat^{cAct}$ mice

We also bred the *Nkx3.1*^{CreERT} mice with *Ctnnb1*$^{lox(ex3)}$ mice. In this model, exon 3 of β-catenin is floxed, and after Cre recombination occurs, a constitutively active version (which is unable to be phosphorylated and degraded) is expressed at high levels. We will refer to this mouse model as $Bcat^{cAct}$. Previously, we have shown that activation of *Ctnnb1*$^{lox(ex3)}$ using the *PB*^{Cre4} promoter resulted in HGPIN [13]. Similar to the Apc^{cKO} mice, no hyperplastic phenotype was observed in the castrated $Bcat^{cAct}$ mice after treatment with tamoxifen or hormonal regeneration alone (Figure 7), following the timeline shown in Figure 4a. There was also no observed phenotype in *Nkx3.1*$^{creERTtg/+}$*Ctnnb1*^{wt} ($Bcat^{wt}$) mice treated with tamoxifen and hormonal regeneration (Figure 7). Prostates from hormonally regenerated $Bcat^{cAct}$ mice displayed HGPIN histology (Figure 7), with evidence of nucleolar enlargement in a subset of cells, as well as more nuclear atypia relative to the Apc^{cKO} mice (data not shown). Prostates from hormonally regenerated $Bcat^{cAct}$ mice also displayed nuclear and cytoplasmic accumulation of β-catenin (Figure 8). As a result of androgen supplement to the control and $Bcat^{cAct}$ mice, prostates derived from these hormonally regenerated mice displayed nuclear staining of AR (Figure 8). Active cell proliferation was observed in the prostatic epithelial cells as shown by Ki67 IHC (Figure 8).

While only a few cells (~1%) in control mice showed positive Ki67 staining, significantly more proliferating cells were seen in prostates derived from hormonally regenerated $Bcat^{cAct}$ mice (Ki67-positive cells: 43% in AP and 15% in DLP). The differences seen in Ki67 positivity between the Apc^{cKO} and $Bcat^{cAct}$ mice (18% versus 43% respectively) may be due to a higher level of active β-catenin in the $Bcat^{cAct}$ mice.

Discussion

In metastatic castration-resistant prostate cancer, mutations have been detected in multiple genes of the Wnt/β-catenin signaling pathway [40]. Studies indicate that Wnt/β-catenin signaling can be activated in prostate cancer via a number of mechanisms in addition to mutation, such as cross-talk with the PTEN/Akt, COX-2/PGE2, TGF-β, and NF-κB pathways [41-43]. Furthermore, reactive stroma is associated with prostate cancer in the microenvironment, and there is increasing evidence indicating that Wnt/β-catenin can also be activated by growth factors and inflammatory factors secreted by fibroblasts and macrophages from the tumor microenvironment [42, 44]. Thus, in addition to the presence of activating mutations in the β-catenin gene and hypermethylation of the Apc gene promoter, a variety of mechanisms can result in activation of β-catenin in human prostate cancer. Consistent with this, human studies found that increased nuclear β-catenin, an indicator of active Wnt signaling, is strongly correlated with advanced-stage prostate cancer and recurrence [45], suggesting that active Wnt/β-catenin signaling would endow prostate cancer cells with a selective advantage during tumor progression.

In this study, we investigated the role of Wnt/β-catenin activation via Apc knockout or constitutive activation of β-catenin in a luminal epithelial prostate cell population. This differs from our previous studies due to the Cre strategy we used ($Nkx3.1^{CreERT}$ versus PB^{Cre4}), as well as the hormonal stages we investigated. We show here that loss of Apc in tamoxifen treated, hormonally normal mice induces HGPIN, correlating with increased active cytoplasmic and nuclear β-catenin levels. These findings are consistent with our previous publication [21], even though Apc is being knocked out in fewer luminal cells (see Figure 1g). Furthermore, these studies show that loss of Apc in prostate luminal cells from sexually mature mice can drive tumorigenesis (as opposed to the Probasin-Cre model in which deletion begins upon the initial exposure to androgen during puberty).

We show that loss of Apc in castrated and hormonally regenerated mice has little effect, which is different than what was observed after loss of Pten in the same model system. The differences could be due to the tumor suppressor being knocked out, rather than the model being used. While loss of Pten in the CARN population causes proliferation and carcinoma, loss of Apc does not increase proliferation after hormonal regeneration, while not reversing the inherent castration resistance. However, we also show that upon constitutive activation of β-catenin under hormonal regeneration conditions, proliferation and PIN result. This could be due to the levels of active β-catenin in the two models, as it was apparent that there was considerably more β-catenin in $Bcat^{cAct}$ mice than in Apc^{cKO} mice. It is also possible that the difference seen between the two models is due to non-β-catenin-related events, such as the interaction and stabilization of microtubule ends by Apc [46]. This will be important to determine, as the CARN provides a paradigm-shifting idea about prostate stem cells. The

role of Wnt signaling, as a primarily developmental pathway in the CARN population, may have far-reaching implications.

Conclusions

We conclude that activation of Wnt/β-catenin signaling alone cannot cause prostate cancer in mice, particularly in the CARN population. Wnt/β-catenin signaling activation alone does cause HGPIN, however, either in a model of Apc deletion or by direct β-catenin activation. A second genetic hit is likely necessary to cause progression to carcinoma and metastasis. Wnt/β-catenin signaling activation acting as a second genetic hit could also cause progression to carcinoma and metastasis, as has been shown previously [14]. In addition, it is possible that repeated rounds of castration and hormonal regeneration could result in loss of Apc-null CARN cells, as shown in our data. What this means in the clinical setting is unclear.

Supplementary Material

Refer to Web version on PubMed Central for supplementary material.

Acknowledgments

We thank Drs. Michael Shen and Corey Abate-Shen for providing mice. We thank Drs. Wade Bushman, Cindy Miranti, and Matt Steensma for advice and discussion. We thank the VARI vivarium and histology cores for their assistance and expertise. We appreciate David Nadziejka's review and technical editing of the manuscript. RJK and XY were funded by NIDDK grant 5RO1 DK055748-14, and BOW and KCV were funded by internal funds from the Van Andel Research Institute.

References Cited

1. American Cancer Society, Inc.. Cancer Facts & Figures. Atlanta: 2011. http://www.cancer.org/Research/CancerFactsFigures/index
2. Valkenburg KC, Williams BO. Mouse Models of Prostate Cancer. Prostate Cancer. 2011; 2011:1–22.
3. Vishnu P, Tan WW. Update on options for treatment of metastatic castration-resistant prostate cancer. Onco Targets Ther. 2010; 3:39–51. [PubMed: 20616956]
4. Lapointe J, Li C, Higgins JP, van de Rijn M, Bair E, Montgomery K, Ferrari M, Egevad L, Rayford W, Bergerheim U, Ekman P, DeMarzo AM, Tibshirani R, Botstein D, Brown PO, Brooks JD, Pollack JR. Gene expression profiling identifies clinically relevant subtypes of prostate cancer. Proc Natl Acad Sci U S A. 2004; 101:811–816. [PubMed: 14711987]
5. Shen MM, Abate-Shen C. Molecular genetics of prostate cancer: new prospects for old challenges. Genes Dev. 2010; 24:1967–2000. [PubMed: 20844012]
6. Zhang TJ, Hoffman BG, Ruiz de Algara T, Helgason CD. SAGE reveals expression of Wnt signalling pathway members during mouse prostate development. Gene Expr Patterns. 2006; 6:310–324. [PubMed: 16378759]
7. Simons BW, Hurley PJ, Huang Z, Ross AE, Miller R, Marchionni L, Berman DM, Schaeffer EM. Wnt signaling though beta-catenin is required for prostate lineage specification. Dev Biol. 2012; 371:246–255. [PubMed: 22960283]
8. Mehta V, Abler LL, Keil KP, Schmitz CT, Joshi PS, Vezina CM. Atlas of Wnt and R-spondin gene expression in the developing male mouse lower urogenital tract. Dev Dyn. 2011; 240:2548–2560. [PubMed: 21936019]
9. Nusse R. Wnt signaling in disease and in development. Cell Res. 2005; 15:28–32. [PubMed: 15686623]

10. Valkenburg KC, Graveel CR, Zylstra-Diegel CR, Zhong Z, Williams BO. Wnt/beta-catenin Signaling in Normal and Cancer Stem Cells. Cancers. 2011; 3:2050–2079. [PubMed: 24212796]
11. Yardy GW, Brewster SF. Wnt signalling and prostate cancer. Prostate Cancer Prostatic Dis. 2005; 8:119–126. [PubMed: 15809669]
12. Chen G, Shukeir N, Potti A, Sircar K, Aprikian A, Goltzman D, Rabbani SA. Up-regulation of Wnt-1 and beta-catenin production in patients with advanced metastatic prostate carcinoma: potential pathogenetic and prognostic implications. Cancer. 2004; 101:1345–1356. [PubMed: 15316903]
13. Yu X, Wang Y, Jiang M, Bierie B, Roy-Burman P, Shen MM, Taketo MM, Wills M, Matusik RJ. Activation of beta-Catenin in mouse prostate causes HGPIN and continuous prostate growth after castration. Prostate. 2009; 69:249–262. [PubMed: 18991257]
14. Yu X, Wang Y, DeGraff DJ, Wills ML, Matusik RJ. Wnt/beta-catenin activation promotes prostate tumor progression in a mouse model. Oncogene. 2011; 30:1868–1879. [PubMed: 21151173]
15. Shoemaker AR, Gould KA, Luongo C, Moser AR, Dove WF. Studies of neoplasia in the Min mouse. Biochim Biophys Acta. 1997; 1332:F25–48. [PubMed: 9141462]
16. Brewster SF, Browne S, Brown KW. Somatic allelic loss at the DCC, APC, nm23-H1 and p53 tumor suppressor gene loci in human prostatic carcinoma. J Urol. 1994; 151:1073–1077. [PubMed: 7510345]
17. Gerstein AV, Almeida TA, Zhao G, Chess E, Shih Ie M, Buhler K, Pienta K, Rubin MA, Vessella R, Papadopoulos N. APC/CTNNB1 (beta-catenin) pathway alterations in human prostate cancers. Genes Chromosomes Cancer. 2002; 34:9–16. [PubMed: 11921277]
18. Watanabe M, Kakiuchi H, Kato H, Shiraishi T, Yatani R, Sugimura T, Nagao M. APC gene mutations in human prostate cancer. Jpn J Clin Oncol. 1996; 26:77–81. [PubMed: 8609698]
19. Richiardi L, Fiano V, Vizzini L, De Marco L, Delsedime L, Akre O, Tos AG, Merletti F. Promoter methylation in APC, RUNX3, and GSTP1 and mortality in prostate cancer patients. J Clin Oncol. 2009; 27:3161–3168. [PubMed: 19470943]
20. Chen Y, Li J, Yu X, Li S, Zhang X, Mo Z, Hu Y. APC gene hypermethylation and prostate cancer: a systematic review and meta-analysis. Eur J Hum Genet. 2013
21. Bruxvoort KJ, Charbonneau HM, Giambernardi TA, Goolsby JC, Qian CN, Zylstra CR, Robinson DR, Roy-Burman P, Shaw AK, Buckner-Berghuis BD, Sigler RE, Resau JH, Sullivan R, Bushman W, Williams BO. Inactivation of Apc in the mouse prostate causes prostate carcinoma. Cancer Res. 2007; 67:2490–2496. [PubMed: 17363566]
22. Goldstein AS, Huang J, Guo C, Garraway IP, Witte ON. Identification of a cell of origin for human prostate cancer. Science. 2010; 329:568–571. [PubMed: 20671189]
23. Wang X, Kruithof-de Julio M, Economides KD, Walker D, Yu H, Halili MV, Hu YP, Price SM, Abate-Shen C, Shen MM. A luminal epithelial stem cell that is a cell of origin for prostate cancer. Nature. 2009; 461:495–500. [PubMed: 19741607]
24. Lawson DA, Xin L, Lukacs RU, Cheng D, Witte ON. Isolation and functional characterization of murine prostate stem cells. Proc Natl Acad Sci U S A. 2007; 104:181–186. [PubMed: 17185413]
25. Choi N, Zhang B, Zhang L, Ittmann M, Xin L. Adult murine prostate basal and luminal cells are self-sustained lineages that can both serve as targets for prostate cancer initiation. Cancer Cell. 2012; 21:253–265. [PubMed: 22340597]
26. Harada N, Tamai Y, Ishikawa T, Sauer B, Takaku K, Oshima M, Taketo MM. Intestinal polyposis in mice with a dominant stable mutation of the beta-catenin gene. EMBO J. 1999; 18:5931–5942. [PubMed: 10545105]
27. Muzumdar MD, Tasic B, Miyamichi K, Li L, Luo L. A global double-fluorescent Cre reporter mouse. Genesis. 2007; 45:593–605. [PubMed: 17868096]
28. Wu X, Wu J, Huang J, Powell WC, Zhang J, Matusik RJ, Sangiorgi FO, Maxson RE, Sucov HM, Roy-Burman P. Generation of a prostate epithelial cell-specific Cre transgenic mouse model for tissue-specific gene ablation. Mech Dev. 2001; 101:61–69. [PubMed: 11231059]
29. Truett GE, Heeger P, Mynatt RL, Truett AA, Walker JA, Warman ML. Preparation of PCR-quality mouse genomic DNA with hot sodium hydroxide and tris (HotSHOT). Biotechniques. 2000; 29:52, 54. [PubMed: 10907076]

30. Qian CN, Knol J, Igarashi P, Lin F, Zylstra U, Teh BT, Williams BO. Cystic renal neoplasia following conditional inactivation of apc in mouse renal tubular epithelium. J Biol Chem. 2005; 280:3938–3945. [PubMed: 15550389]

31. Hu WY, Shi GB, Lam HM, Hu DP, Ho SM, Madueke IC, Kajdacsy-Balla A, Prins GS. Estrogen-initiated transformation of prostate epithelium derived from normal human prostate stem-progenitor cells. Endocrinology. 2011; 152:2150–2163. [PubMed: 21427218]

32. Bhatia-Gaur R, Donjacour AA, Sciavolino PJ, Kim M, Desai N, Young P, Norton CR, Gridley T, Cardiff RD, Cunha GR, Abate-Shen C, Shen MM. Roles for Nkx3.1 in prostate development and cancer. Genes Dev. 1999; 13:966–977. [PubMed: 10215624]

33. Kim MJ, Cardiff RD, Desai N, Banach-Petrosky WA, Parsons R, Shen MM, Abate-Shen C. Cooperativity of Nkx3.1 and Pten loss of function in a mouse model of prostate carcinogenesis. Proc Natl Acad Sci U S A. 2002; 99:2884–2889. [PubMed: 11854455]

34. Ittmann M, Huang J, Radaelli E, Martin P, Signoretti S, Sullivan R, Simons BW, Ward JM, Robinson BD, Chu GC, Loda M, Thomas G, Borowsky A, Cardiff RD. Animal models of human prostate cancer: the consensus report of the New York meeting of the Mouse Models of Human Cancers Consortium Prostate Pathology Committee. Cancer Res. 2013; 73:2718–2736. [PubMed: 23610450]

35. Mirosevich J, Gao N, Matusik RJ. Expression of Foxa transcription factors in the developing and adult murine prostate. Prostate. 2005; 62:339–352. [PubMed: 15389796]

36. Wu X, Daniels G, Shapiro E, Xu K, Huang H, Li Y, Logan S, Greco MA, Peng Y, Monaco ME, Melamed J, Lepor H, Grishina I, Lee P. LEF1 identifies androgen-independent epithelium in the developing prostate. Mol Endocrinol. 2011; 25:1018–1026. [PubMed: 21527502]

37. Zhao B, Lei QY, Guan KL. The Hippo-YAP pathway: new connections between regulation of organ size and cancer. Curr Opin Cell Biol. 2008; 20:638–646. [PubMed: 18955139]

38. Azzolin L, Zanconato F, Bresolin S, Forcato M, Basso G, Bicciato S, Cordenonsi M, Piccolo S. Role of TAZ as mediator of Wnt signaling. Cell. 2012; 151:1443–1456. [PubMed: 23245942]

39. Lei QY, Zhang H, Zhao B, Zha ZY, Bai F, Pei XH, Zhao S, Xiong Y, Guan KL. TAZ promotes cell proliferation and epithelial-mesenchymal transition and is inhibited by the hippo pathway. Mol Cell Biol. 2008; 28:2426–2436. [PubMed: 18227151]

40. Grasso CS, Wu YM, Robinson DR, Cao X, Dhanasekaran SM, Khan AP, Quist MJ, Jing X, Lonigro RJ, Brenner JC, Asangani IA, Ateeq B, Chun SY, Siddiqui J, Sam L, Anstett M, Mehra R, Prensner JR, Palanisamy N, Ryslik GA, Vandin F, Raphael BJ, Kunju LP, Rhodes DR, Pienta KJ, Chinnaiyan AM, Tomlins SA. The mutational landscape of lethal castration-resistant prostate cancer. Nature. 2012; 487:239–243. [PubMed: 22722839]

41. Persad S, Troussard AA, McPhee TR, Mulholland DJ, Dedhar S. Tumor suppressor PTEN inhibits nuclear accumulation of beta-catenin and T cell/lymphoid enhancer factor 1-mediated transcriptional activation. J.Cell Biol. 2001; 153:1161–1174. [PubMed: 11402061]

42. Castellone MD, Teramoto H, Williams BO, Druey KM, Gutkind JS. Prostaglandin E2 promotes colon cancer cell growth through a Gs-axin-beta-catenin signaling axis. Science. 2005; 310:1504–1510. [PubMed: 16293724]

43. Carayol N, Wang CY. IKKalpha stabilizes cytosolic beta-catenin by inhibiting both canonical and non-canonical degradation pathways. Cell Signal. 2006; 18:1941–1946. [PubMed: 16616828]

44. Juan J, Muraguchi T, Iezza G, Sears RC, McMahon M. Diminished WNT -> beta-catenin -> c-MYC signaling is a barrier for malignant progression of BRAFV600E-induced lung tumors. Genes Dev. 2014; 28:561–575. [PubMed: 24589553]

45. Yardy GW, Brewster SF. Wnt signalling and prostate cancer. Prostate Cancer Prostatic.Dis. 2005; 8:119–126. [PubMed: 15809669]

46. Barth AI, Siemers KA, Nelson WJ. Dissecting interactions between EB1, microtubules and APC in cortical clusters at the plasma membrane. J Cell Sci. 2002; 115:1583–1590. [PubMed: 11950877]

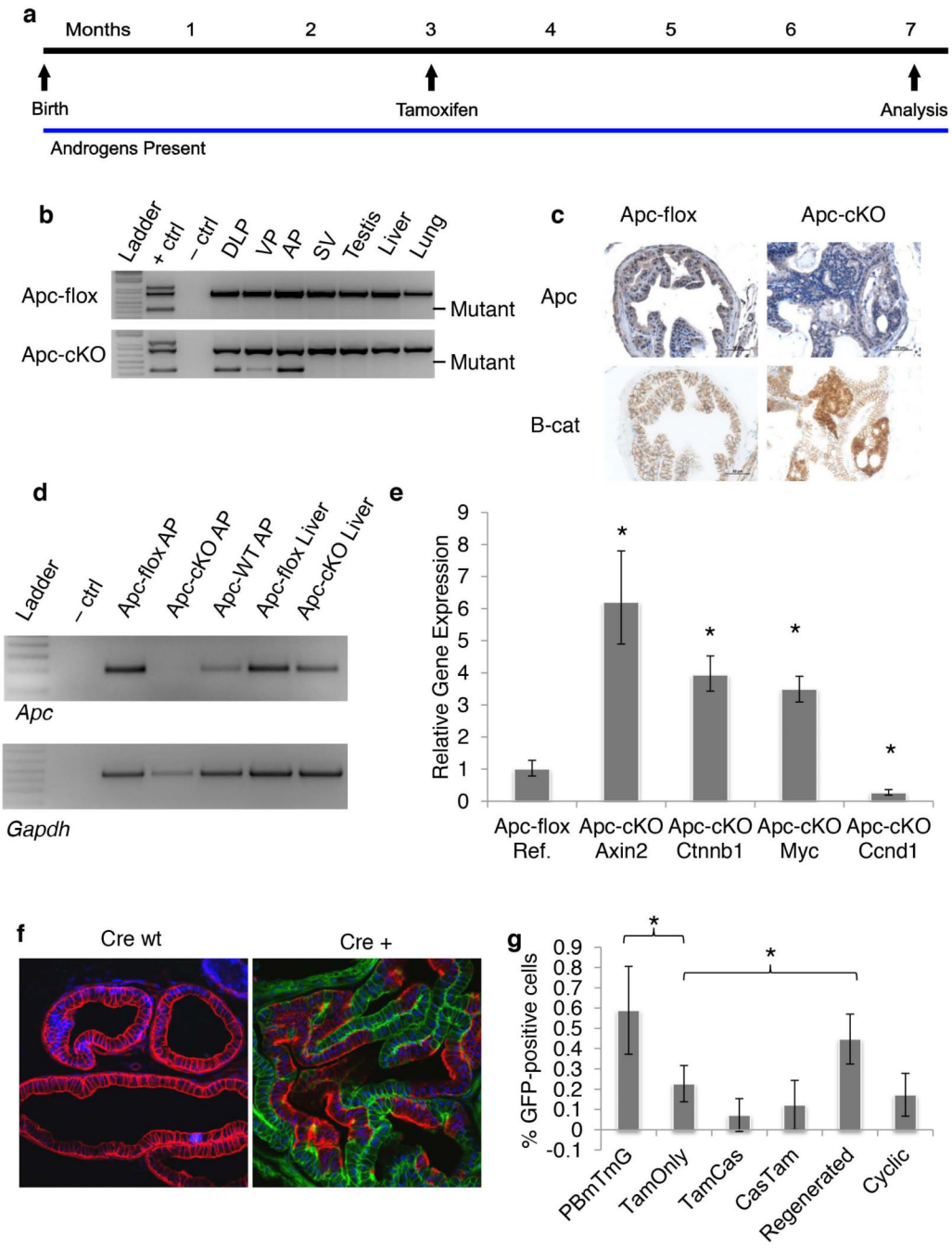

Figure 1. Deletion of Apc induced β-catenin and Axin2 expression

(a) Timeline of tamoxifen treatment for the Tam-only group. (b) *Apc*-allele-specific PCR on tissue from control mice without Cre expression - *Nkx3.1*$^{CreERT+/+}$;*Apc*$^{flox/flox}$ (Apc^{flox}) or *Nkx3.1*$^{CreERTtg/+}$;*Apc*$^{flox/flox}$ (Apc^{cKO}) mice. DLP: dorsolateral prostate; VP: ventral prostate; AP: anterior prostate; SV: seminal vesicle. (c) Apc and β-catenin IHC on anterior prostate tissue from Apc^{flox} or Apc^{cKO} mice. (d) *Apc* qualitative RT-PCR on anterior prostate tissue from Apc^{flox} or Apc^{cKO} mice. (e) Quantitative RT-PCR on anterior prostate tissue from Apc^{flox} or Apc^{cKO} mice; * p <0.0003. (f) Confocal imaging of

Nkx3.1^{CreERT}*mT/mG* anterior prostate. (g) Quantification of GFP-positive cells from *PB*^{Cre4}*mT/mG* (left bar) or *Nkx3.1*^{CreERT}*mT/mG* (remaining bars) anterior prostate. * $p < 0.05$.

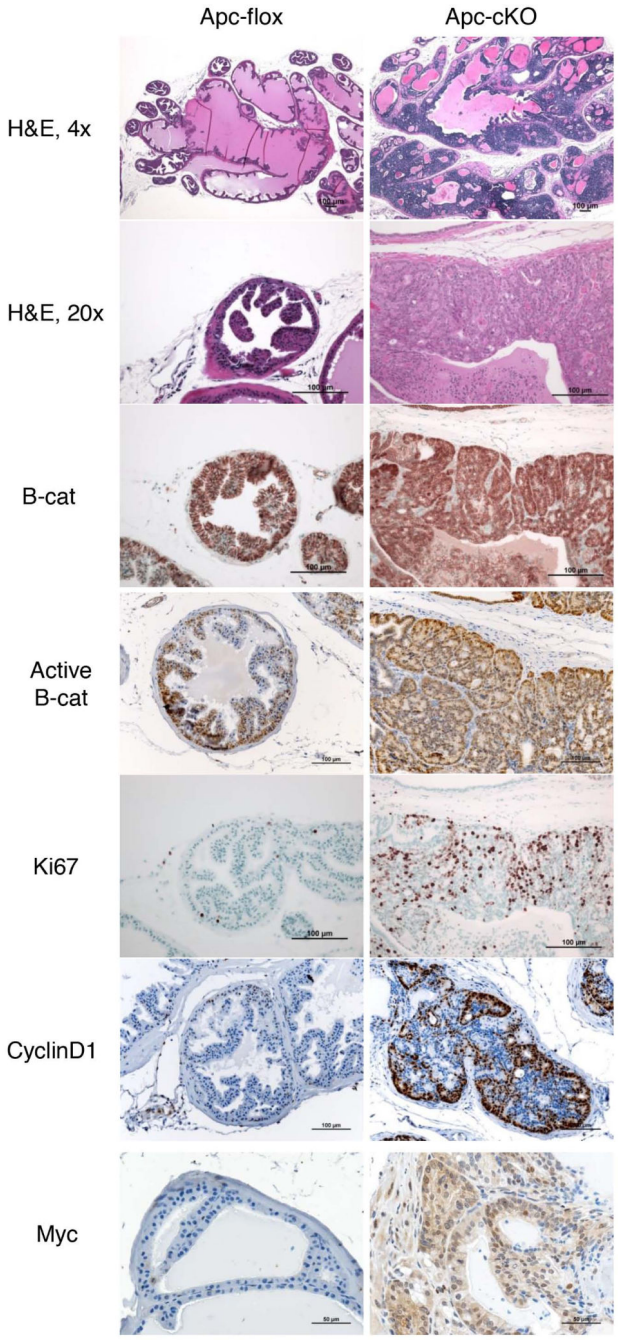

Figure 2. Prostate tissue from Apc^{cKO} mice displayed HGPIN with increased proliferation correlated with increased cytoplasmic and nuclear levels of β-catenin

H&E and IHC staining of anterior prostate tissue from Apc^{flox} and Apc^{cKO} mice at 7 months of age (4 months post-tamoxifen treatment). H&E: hematoxylin and eosin; B-cat: β-catenin IHC; Active B-cat: activated β-catenin IHC (stains for non-phosphorylated version of β-catenin); Ki67; Cyclin D1; and Myc.

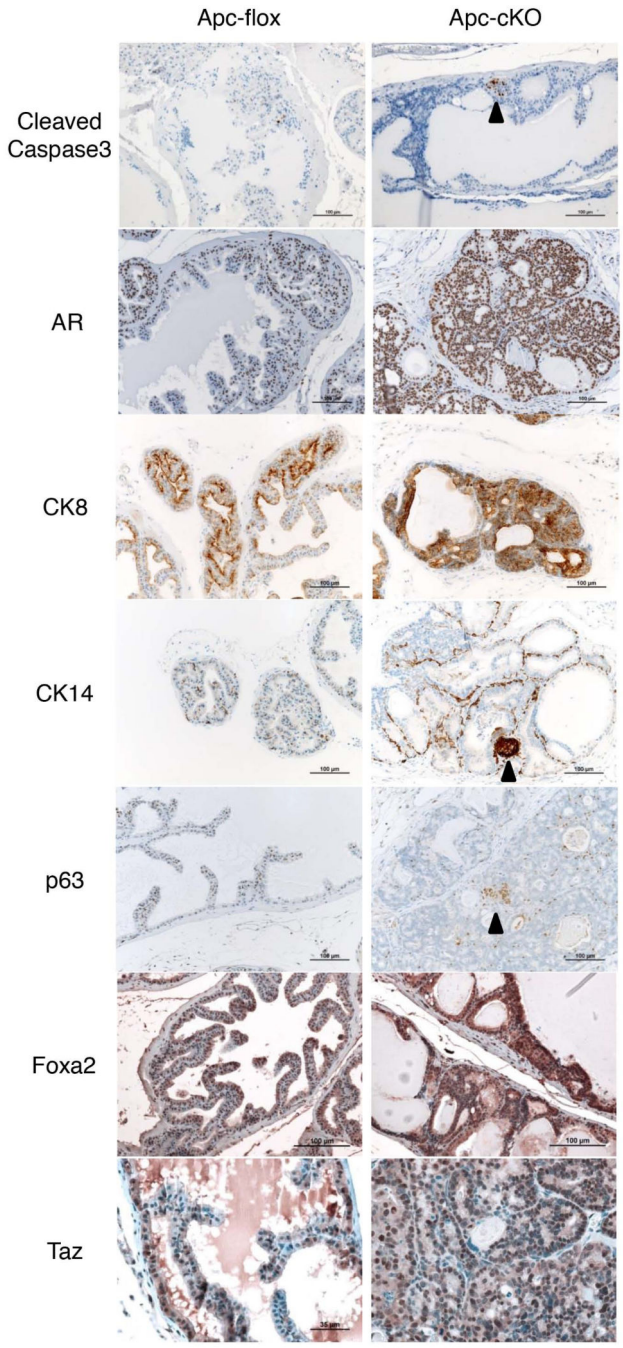

Figure 3. The luminal compartment of Apc^{cKO} mice expressed increased AR and both luminal and basal markers

Staining of anterior prostate tissue from Apc^{flox} and Apc^{cKO} mice at 7 months of age (4 months post-tamoxifen treatment). Cleaved Caspase 3; AR: androgen receptor; CK8: cytokeratin 8; CK14: cytokeratin 14; p63; Foxa2; and Taz.

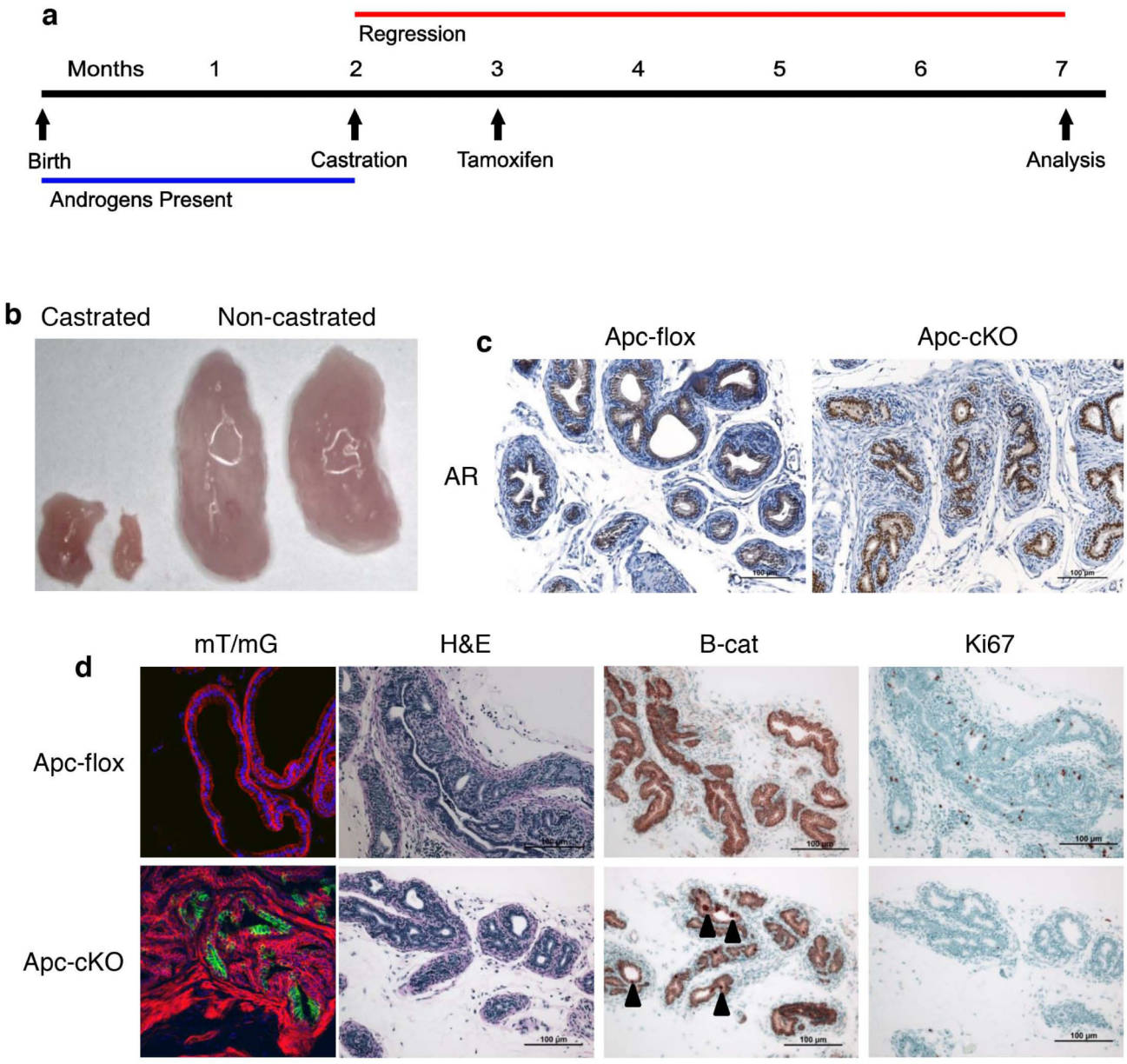

Figure 4. A small population of Apc^{cKO} cells survived castration but did not proliferate

(a) Timeline of tamoxifen treatment and castration for the Cas-Tam group. (b) Anterior prostate lobes from castrated and non-castrated mice. (c) AR IHC on prostate tissue from Apc^{flox} and Apc^{cKO} mice in the Cas-Tam group. (d) Confocal mT/mG imaging of Cas-Tam mice, as well as H&E and β-catenin and Ki67 immunostaining of prostate tissues from Apc^{flox} and Apc^{cKO} mice in the Cas-Tam group.

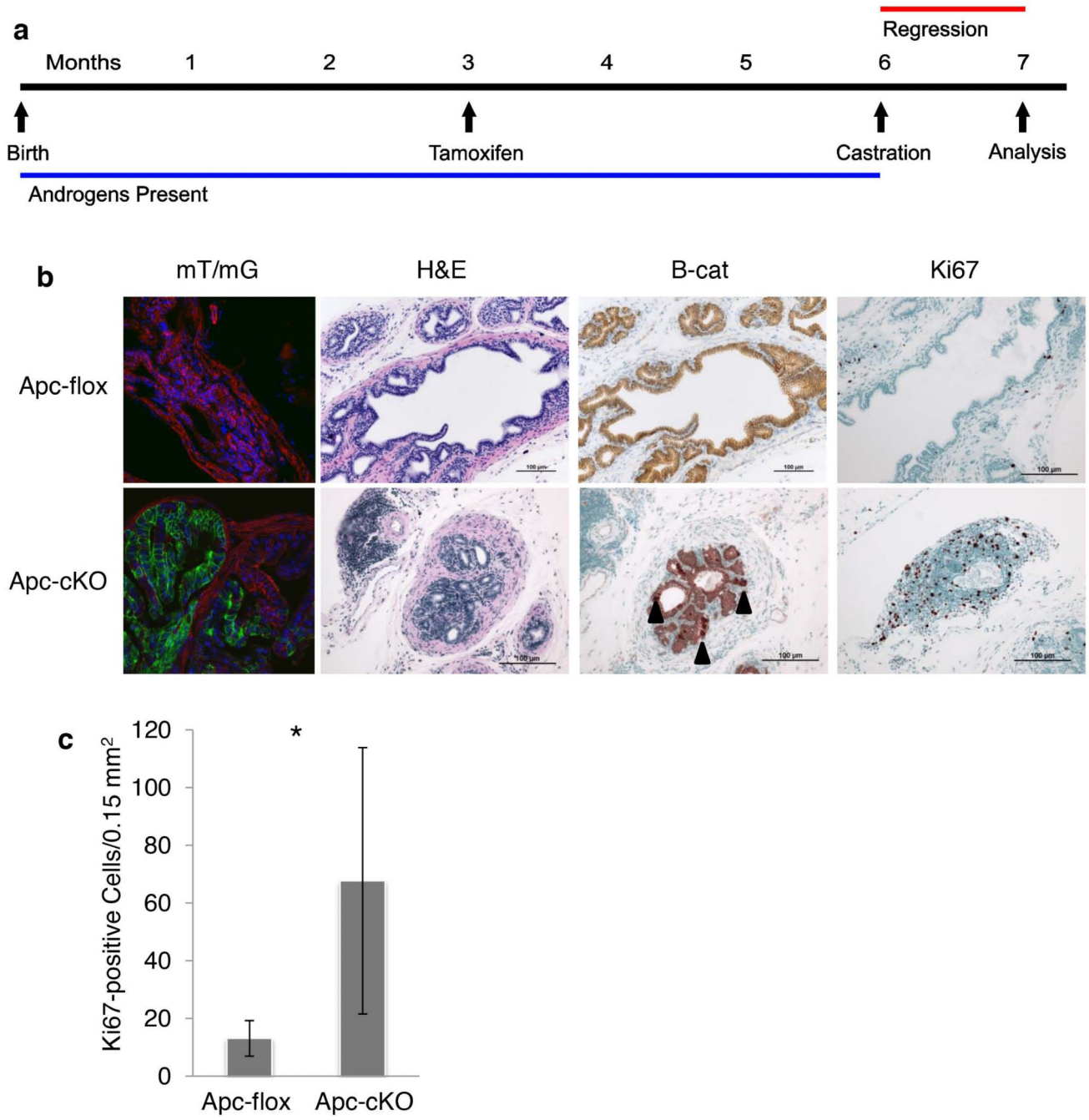

Figure 5. Increased proliferation in Apc^{cKO} mice when castrated after Tamoxifen-induced Cre induction

(a) Timeline of tamoxifen treatment and castration for the Tam-Cas group. (b) Confocal mT/mG imaging for Cas-Tam mice, as well as H&E and β-catenin and Ki67 immunostaining of prostate tissues from Apc^{flox} and Apc^{cKO} mice in the Tam-Cas group. (c) Quantification of Ki67-positive cells in anterior prostate sections from Apc^{flox} and Apc^{cKO} mice; * p = 0.003.

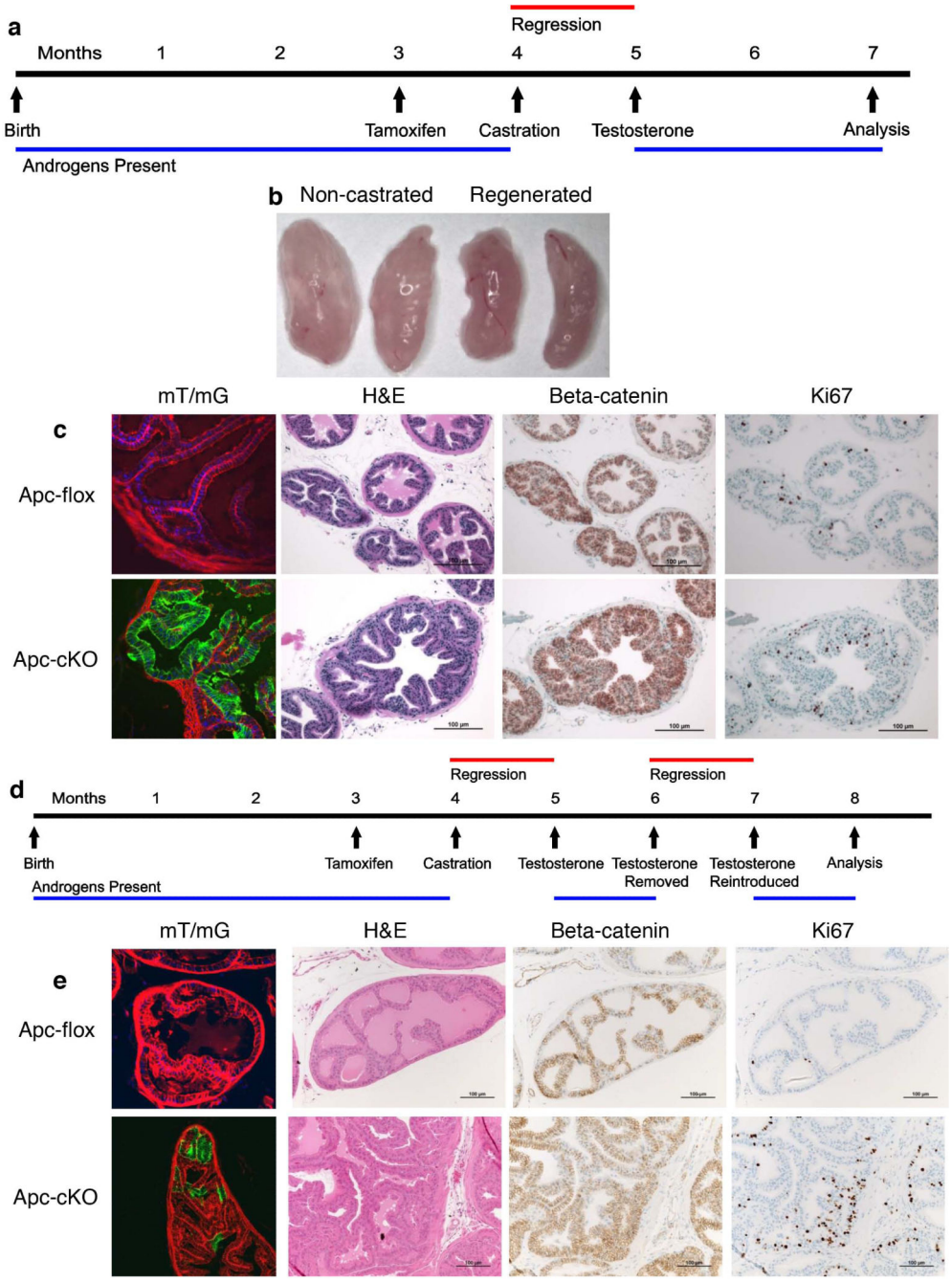

Figure 6. A single or multiple rounds of castration and hormonal regeneration eliminated the Apc^{cKO} cell population

(a) Timeline of tamoxifen treatment, castration, and testosterone treatment for the Regenerated group. (b) Anterior prostate lobes from regenerated and non-castrated mice. (c) Confocal mT/mG imaging for Cas-Tam mice, as well as H&E and β-catenin and Ki67 immunostaining of prostate tissues from Apc^{flox} and Apc^{cKO} mice in the Regenerated group. (d) Diagram of the timeline of tamoxifen treatment, castration, and testosterone treatment for the Cyclic group. (e) Confocal mT/mG imaging for Cas-Tam mice, as well as

H&E and β-catenin and Ki67 immunostaining of prostate tissues from Apc^{flox} and Apc^{cKO} mice in the Cyclic group.

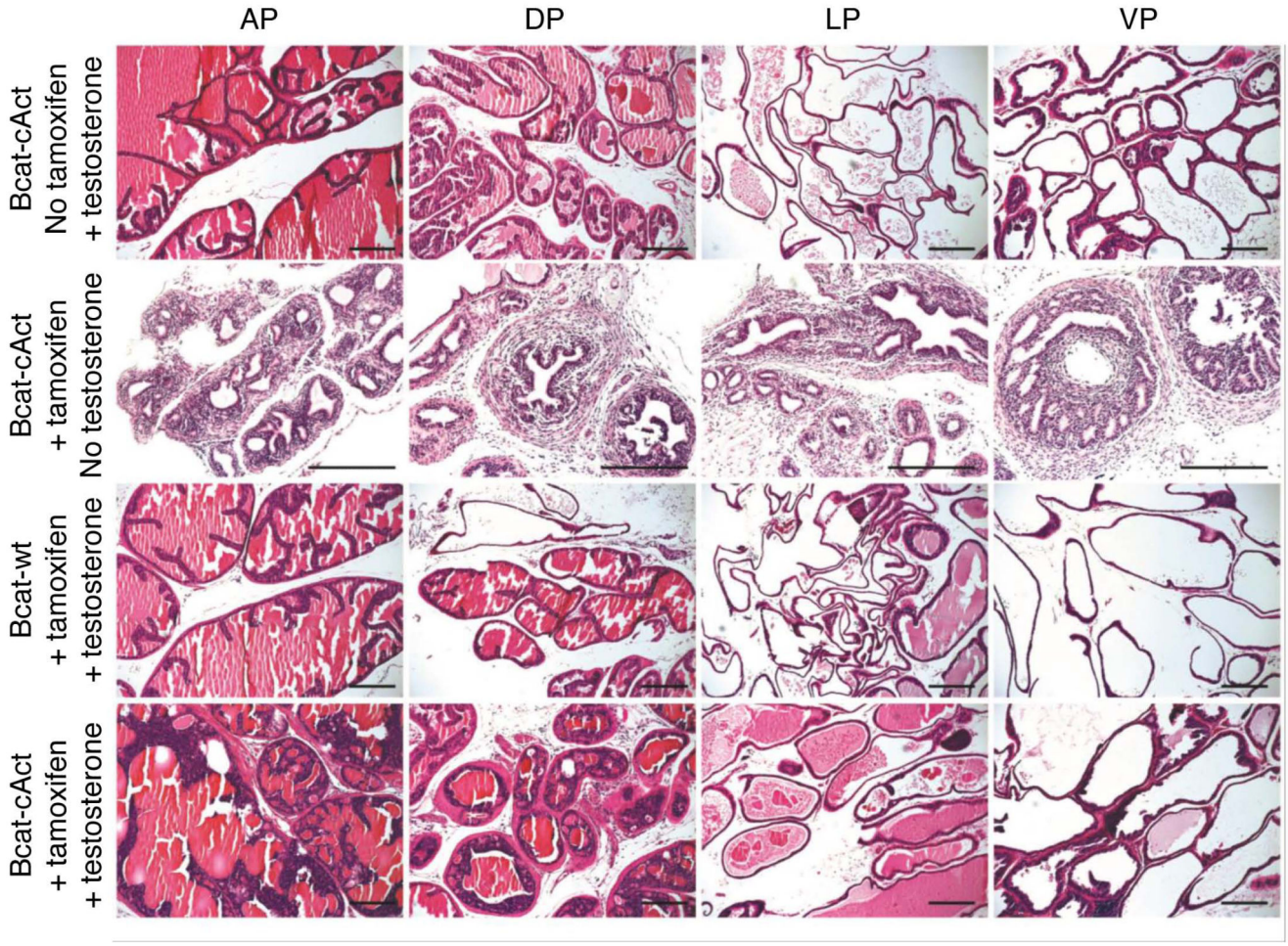

Figure 7. Prostate tissue from Bcat^{cAct} mice displayed PIN after castration and hormonal regeneration

H&E stained prostates from *Nkx3.1*$^{CreERTtg/+}$;*Ctnnb1*$^{+/+}$ (Bcat^{wt}) and *Nkx3.1*$^{CreERTtg/+}$;*Ctnnb1*$^{lox(ex3)}$ (Bcat^{cAct}) mice. All of the mice were castrated. Bars = 100 μm.

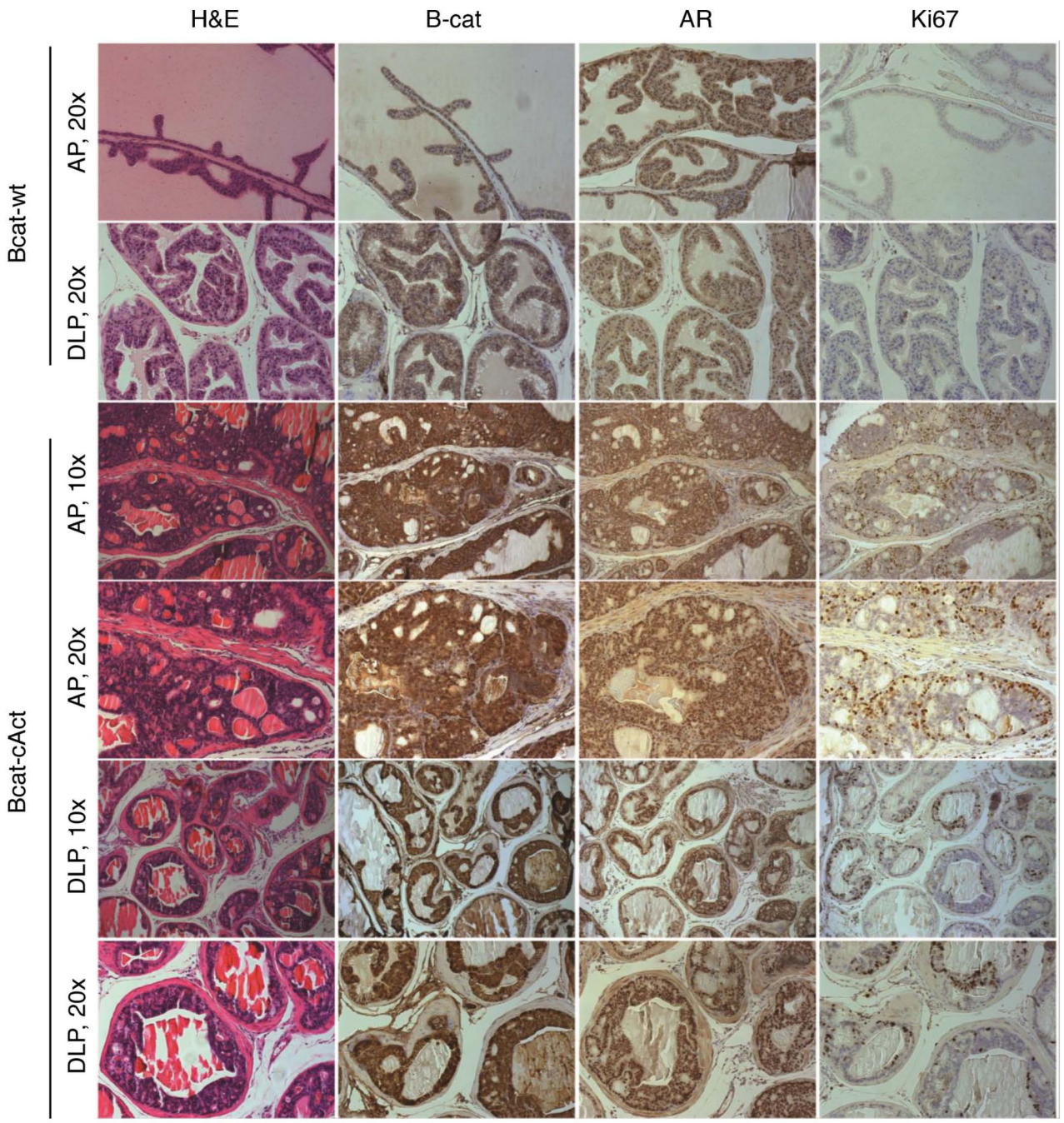

Figure 8. Prostate tissue from Bcat^{cAct} mice displayed HGPIN with increased proliferation correlated with increased cytoplasmic and nuclear levels of β-catenin

Staining of anterior prostate tissue from Bcat^{wt} and Bcat^{cAct} mice at 7 months of age (3 months post-tamoxifen treatment).